BIOINFORMATICS ORIGINAL PAPER Vol. 26 no. 17 2010, pages 2169–2175
doi:10.1093/bioinformatics/btq400

Systems biology

Advance Access publication July 7, 2010

A system-level investigation into the cellular toxic response mechanism mediated by AhR signal transduction pathway

Jungsoo Gim[1,2,†], Ho-Shik Kim[3,†], Junil Kim[1,†], Minsoo Choi[1], Jeong-Rae Kim[1], Yeun Jun Chung[4] and Kwang-Hyun Cho[1,*]

[1]Department of Bio and Brain Engineering, Korea Advanced Institute of Science and Technology (KAIST), 335 Gwahangno, Yuseong-gu, Daejeon 305-701, [2]Interdisciplinary Program in Bioinformatics, Seoul National Univeristy, Gwanak-gu, Seoul 151-747, [3]Department of Biochemistry and [4]Department of Microbiology, College of Medicine, The Catholic University of Korea, Seoul 137-701, Republic of Korea

Associate Editor: Alfonso Valencia

ABSTRACT

Motivation: Viewing a cellular system as a collection of interacting parts can lead to new insights into the complex cellular behavior. In this study, we have investigated aryl hydrocarbon receptor (AhR) signal transduction pathway from such a system-level perspective. AhR detects various xenobiotics, such as drugs or endocrine disruptors (e.g. dioxin), and mediates transcriptional regulation of target genes such as those in the cytochrome P450 (CYP450) family. On binding with 2,3,7,8-tetrachlorodibenzo-p-dioxin (TCDD), however, AhR becomes abnormally activated and conveys toxic effects on cells. Despite many related studies on the TCDD-mediated toxicity, quantitative system-level understanding of how TCDD-mediated toxicity generates various toxic responses is still lacking.

Results: Here, we present a manually curated TCDD-mediated AhR signaling pathway including crosstalks with the hypoxia pathway that copes with oxygen deficiency and the p53 pathway that induces a DNA damage response. Based on the integrated pathway, we have constructed a mathematical model and validated it through quantitative experiments. Using the mathematical model, we have investigated: (i) TCDD dose-dependent effects on AhR target genes; (ii) the crosstalk effect between AhR and hypoxia signals; and (iii) p53 inhibition effect of TCDD-liganded AhR. Our results show that cellular intake of TCDD induces AhR signaling pathway to be abnormally up-regulated and thereby interrupts other signaling pathways. Interruption of hypoxia and p53 pathways, in turn, can incur various hazardous effects on cells. Taken together, our study provides a system-level understanding of how AhR signal mediates various TCDD-induced toxicities under the presence of hypoxia and/or DNA damage in cells.

Contact: ckh@kaist.ac.kr

Supplementary information: Supplementary data are available at *Bioinformatics* online.

Received on October 20, 2009; revised on June 9, 2010; accepted on July 3, 2010

1 INTRODUCTION

Cells are composed of well-organized molecular interaction networks. To understand the response mechanism of a cell against an external stimulation, we should not only identify the mediating signal transduction pathways but also investigate the dynamics accompanied with the signal transmission. This can be readily achieved using high-throughput techniques such as microarray experiments, but previous studies indicated the problem of low reproducibility in such cases (Zhang *et al.*, 2008). So, we construct a mathematical model for computer simulations by employing low-throughput techniques and investigate the dynamics of cell signaling at a system-level by combined analysis of computer simulations and biochemical experimentation. Based on the collection of biological or biochemical information about signaling pathways induced by a specific stimulation, we can construct the relevant molecular interaction network and further investigate the dynamics of the molecules involved in the network (Kim *et al.*, 2007, 2009; Kwon and Cho, 2008; Shin *et al.*, 2008, 2009). This might lead us to a system-level understanding of the complex phenomena. Here, we applied the idea to the AhR signaling pathway to unravel the complicated signaling pathway disruption by external stimulations.

Aryl hydrocarbon receptor (AhR) is a member of the basic helix–loop–helix/Period–aryl hydrocarbon nuclear translocator (ARNT)–Single minded (bHLH/PAS) DNA binding protein family. Although AhR is located in the cytosol bound to a molecular complex composed of HSP90, XAP2 and p23, upon binding with a ligand such as TCDD, it is translocated to the nucleus and becomes heterodimerized with ARNT after dissociated from the HSP90/XAP2/p23 complex. This liganded AhR/ARNT dimer binds to consensus regulatory sequences of DNA, called 'dioxin response elements' or 'xenobiotic response elements' and transcribes the associated genes.

2,3,7,8-Tetrachlorodibenzo-p-dioxin (TCDD) is a specific type of polychlorinated dibenzodioxins, also known as dioxin, which is one group of the most toxic materials including dioxin-like chemicals known so far, such as polychlorinated dibenzofurans and biphenyls. TCDD is used as a toxic standard evaluating the toxic equivalency factor (TEF) value of dioxins and dioxin-like chemicals to indicate the degree of toxicity. TCDD is top ranked with TEF = 1, which is the highest value among the tested chemicals (Van den Berg *et al.*, 1998,

*To whom correspondence should be addressed.

†The authors wish it to be known that, in their opinion, the first three authors should be regarded as joint First Authors.

2006). TCDD is a toxic standard for dioxin-like chemicals because a number of evidences have been reported about its various hazardous effects on human body: liver and skin damages (Kimbrough *et al*., 1977), diabetes (Longnecker and Michalek, 2000), thyroid (Pavuk *et al*., 2003), etc. Recent studies also revealed that TCDD could be a potential carcinogen (Safe, 2001).

Although various toxic effects of TCDD have been studied for several decades, its detailed molecular mechanisms are still poorly understood except the TCDD-mediated transcriptional regulation of AhR and its binding with ARNT. TCDD gets bio-accumulated in fatty tissue of human due to its hydrophobicity with wide individual variation of half-life ∼7–10 years (Geyer *et al*., 2002; Pirkle *et al*., 1989). Accumulated in fatty tissue, TCDD sustains AhR activation and causes the transcription of target genes such as *CYP1A1* (Cytochrome P450, family 1, subfamily A, polypeptide 1) and *AhRR* (AhR repressor gene) (Mimura and Fujii-Kuriyama, 2003). In many cases, the TCDD toxicity is strongly related to the accumulation of CYP1A1. Although there have been a number of studies to discover the downstream mechanism followed by this abnormal accumulation of CYP1A1, it is still unclear how the downstream signals flow and what affects the cellular toxicity.

Conventional studies on toxic materials usually focus on a single particular aspect among various observed toxicities or phenomenological responses, called 'dose–response relationship' in which the dose denotes the amount of a toxic substance and the response usually indicates the lethal rate of an organism. However, complex polygenic disease like cancer and diverse effects of toxic materials on living organisms need a broader *systems* approach.

Several recent studies revealed that AhR may crosstalk with other signaling pathways so that liganded AhR could affect other biological functions (Gradin *et al*., 1996; Paajarvi *et al*., 2005). In particular, we note two previous studies reporting that TCDD-liganded AhR inactivates p53 by increasing the basal level of MDM2 protein, not its *m*RNA, which is a well-known E3 ubiquitin ligase (Paajarvi *et al*., 2005) and ARNT, the counterpart of AhR, binds with hypoxia inducible factor 1 alpha (HIF1α), a well-known hypoxia responding protein (Gradin *et al*., 1996; Pollenz *et al*., 1999). ARNT is one of the bHLH/PAS transcription factor families. ARNT transcribes various genes after binding with HIF1α (or AhR) to cope with toxic perturbations such as hypoxia (or dioxin intake). This suggests the possibility that ARNT might play a limiting role in the competing signal transmission between AhR and HIFs (Reisdorph and Lindahl, 2001). These results indicate that TCDD might have some positive effect on carcinogenesis by disturbing the DNA damage response signaling pathways and the role of p53, and negative effect by competing with HIF1α that transcribes genes related to angiogenesis under hypoxia. Hence, there is a pressing need to do a system-level study on these such that we can unravel the molecular mechanism of various toxic responses produced by the TCDD-mediated AhR signaling pathway.

2 BACKGROUND

TCDD intake is related to the regulation of P53, a well-known tumor suppressor gene and an important element in anti-cancer mechanism. In normal cells, the basal level of p53 protein is low due to the regulation by its ubiquitin ligase, MDM2. If DNA damage occurs (DNA damage frequently occurs in cells because of ultraviolet ray, reactive oxygen species, etc.), MDM2 becomes inactive and thereby p53 gets accumulated. Then, a set of genes are transcribed that are related to cell-cycle arrest, DNA repair and apoptosis, to cope with the damage (Harris and Levine, 2005). It is intriguing that MDM2 is also transcribed by p53 and that this forms the p53-MDM2 negative feedback loop.

The dynamics of the p53-MDM2 feedback loop in individual cells has been intensively investigated in several studies (Geva-Zatorsky *et al*., 2006; Lahav *et al*., 2004; Zhang *et al*., 2007). In particular, Alon and his colleagues discovered that p53 shows an increased number of repeated pulse expressions in response to the DNA damage (Geva-Zatorsky *et al*., 2006; Lahav *et al*., 2004). Based on these studies, Zhang *et al.* (2007) proposed a mathematical model by assuming that p53 goes through conformational changes depending on its particular transcriptional activity: p53-killer transcribes genes related to apoptosis and p53-helper transcribes genes related to cell-cycle arrest or DNA repair. In this model, a transient form between p53-helper and p53-killer is also assumed and denoted as p53-lurker (Zhang *et al*., 2007).

3 MATERIALS AND METHODS

3.1 Model construction

We have surveyed KEGG (Kanehisa and Goto, 2000) database as well as all the relevant literature to construct a manually curated AhR signaling pathway. Using all possible combinations of 'AhR', 'TCDD', 'hypoxia', 'p53' and 'crosstalk' as queries, we found the most relevant 107 articles and used them to construct a reaction diagram that is largely composed of three different modules (AhR, hypoxia and p53 module; Fig. 1). Then, we have constructed a mathematical model of it using ordinary differential equations (ODEs) based on the mass action law for protein interactions (Cho *et al*., 2003) and the saturating rate law for transcriptional reactions in the reaction diagram. For instance, for a given protein interactions

$$A+B+\cdots \underset{k_{-1}}{\overset{k_1}{\rightleftarrows}} C+D+\cdots,$$

the changing rate of protein A with respect to time can be described as

$$\frac{\mathrm{d}[A]}{\mathrm{d}t} = -k_1[A][B][\cdots]+k_{-1}[C][D][\cdots],$$

where $[A]$ denotes the concentration of protein A and k_1 and k_{-1} represent the rate constants for forward and backward reactions, respectively. Transcriptional activation and inhibitory reactions were modeled using Hill-type functions (Kim,J.R. *et al*., 2008)

$$\begin{pmatrix} \frac{V\times[\mathrm{A}]^n}{K^n+[A]^n} \\ \frac{V}{K^n+[A]^n} \end{pmatrix} \sim \begin{pmatrix} \text{Activation} \\ \text{Inhibition} \end{pmatrix},$$

where V, K, n denote the rate constant, the dissociation constant and the Hill coefficient, respectively. The model contains 67 reactions (61 from manual curation and 6 from KEGG). The details of the ODE model are summarized in Supplementary Material.

3.2 Parameter estimation

For simulations, parameter values were adopted from literature if they are available, and all the remaining parameter values were estimated from our own experiments using the genetic algorithm (GA):

(1) Construct 500 chromosomes (initial chromosomes) composed of 43 random numbers within a range between 0.01 and 100.

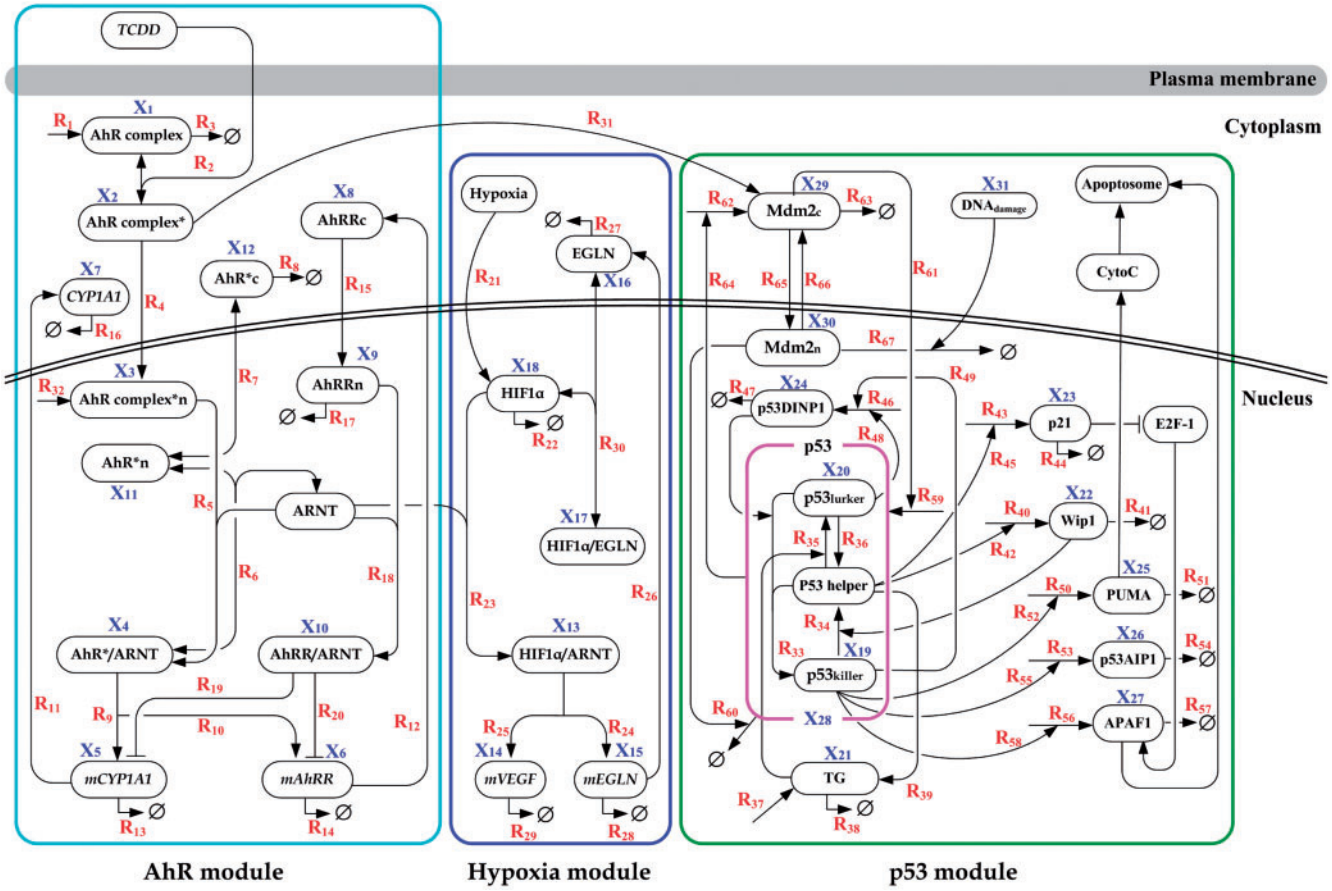

Fig. 1. A circuit diagram of TCDD-mediated AhR pathway. The pathway is composed of three interconnected modules: AhR, hypoxia and p53 modules. TCDD-liganded AhR transduces a signal to both AhR and p53 modules, and has a crosstalk with HIF1α signal. X_i and R_i denote the i-th molecular component and the i-th reaction, respectively. See Supplementary Material for all the equations and reactions in detail.

(2) Evaluate the fitness of each chromosome using the fitness:

$$Fitness = \frac{100}{\sqrt{\sum_{i=1}^{n}(s_i - e_i)^2}}$$

where n is the number of sampling time points, s_i the simulated data at the i-th sampling time and e_i the experimental data at the i-th sampling time.

(3) Select 2 parent chromosomes out of 500 chromosomes with the selection rate proportional to their fitness.

(4) Decide whether to apply crossover to the parent chromosomes with the crossover rate 0.68 (see Kim,J. *et al*., 2008, for details). If a random number generated between 0 and 1 is less than the crossover rate, produce a pair of child chromosomes by dividing each chromosome of the parent pairs at random positions and swapping each segment of the divided chromosomes. Otherwise, the two parent chromosomes will be used as child chromosomes without any change.

(5) Make 500 child chromosomes by repeating from (4) to (5) for 250 times.

(6) Randomly mutate the selected numbers of each child chromosome with the mutation rate 0.03 (see Kim,J. *et al*., 2008, for details) for each number.

(7) Evaluate the fitness of each child chromosome and replace the child chromosome having the worst fitness with the parent chromosome having the best fitness.

(8) Repeat from (4) to (8) for 1000 times.

Regarding the p53 module, we have employed the model proposed by (Zhang *et al*., 2007). All the variables, reactions, and parameters used in the model can be found in Supplementary Tables S1–3, respectively. The experimental data used to fit the model are summarized in Supplementary Table S4.

3.3 Materials and antibodies

TCDD was purchased from AccuStandard (New Haven, CT, USA). Toluene contained in TCDD stock solution was evaporated and TCDD was re-dissolved in DMSO (Sigma, St Louis, MO, USA) for treatment to cells. Anti-AhR and anti-glyceraldehyde-3-phosphate dehydrogenase (anti-GAPDH) were obtained from Santa Cruz Biotechonology (Santa Cruz, CA, USA). Anti-CYP1A1 and anti-phospho-p53 (Ser-15) were from Biomol (Plymouth meeting, PA, USA) and cell-signaling technology, INC. (Danvers, MA, USA), respectively.

3.4 Cell culture

HepG2 cells obtained from American Type Culture Collection were maintained in high glucose Dulbecco's Modified Eagle Medium (DMEM,

Invitrogen, Carlsbad, CA, USA) supplemented with 10% fetal bovine serum (FBS, Hyclone, Logan, UT, USA) and penicillin/streptomycin (Sigma).

3.5 Quantitative real time polymerase chain reaction (RT–PCR)

RNA was extracted using RNA STAT60 (Tel-test, Friendswood, TX, USA) from cells treated with indicated concentrations of TCDD for indicated periods and subjected to complementary DNA synthesis using AccuPowerCycleScript RT Premix (Bioneer, Daejon, Korea). The real-time RT–PCR was performed with mixtures containing synthesized cDNA, 1× SYBR premix Ex Taq (TaKaRa Bio Inc, Shiga, Japan), 0.5× ROX and primers using Mx3000P quantitative polymerase chain reaction (QPCR) (Stratagene, La Jolla, CA, USA). GAPDH was used as an internal control in each procedure. The thermal cycling was one cycle at 95°C for 2 min, followed by 40 cycles of 95°C at 10 s and 60°C for 30 s. After amplifying reaction, melting curve analysis was performed from 55°C to 95°C(Δ0.5°C/s). Relative quantification was analyzed by the ΔΔCt method (Livak and Schmittgen, 2001). The sequences of primers against CYP1A1, GAPDH and VEGFα were as follows:

CYP1A1
Forward primer, 5′-ATTATCTTTGGCATGGGCAAGCGG-3′
Reverse primer, 5′-CAGCTGCATTTGGAAGTGCTCACA-3′
GAPDH
Forward primer, 5′-TCGACAGTCAGCCGCATCTTCTTT-3′
Reverse primer, 5′-ACCAAATCCGTTGACTCCGACCTT-3′
VEGFα
Forward primer, 5′-TTTCTGCTGTCTTGGGTGCATTGG-3′
Reverse primer, 5′-ACCACTTCGTGATGATTCTGCCCT-3′

3.6 Immunoblot analysis

Proteins extracted from TCDD-treated cells were subjected to 10% SDS–PAGE. Separated proteins were electrically transferred to nitrocellulose membranes. Nitrocellulose membranes were soaked in 5% non-fat dried milk for 30 min and then incubated with primary antibodies for overnight at 4°C. After being washed, membranes were incubated with horseradish peroxidase-conjugated secondary antibodies at room temperature. An hour later, membranes were washed in tris-tween buffered saline (TTBS) and proteins were detected by enhanced chemiluminescence kit (Amersham, Buckinghamshire, UK) according to the manufacturer's instructions.

4 RESULTS AND DISCUSSION

4.1 A system-level reconstruction of the TCDD-mediated AhR signaling pathway

To have a system-level understanding of AhR signaling, we have collected all the relevant molecular interaction information from both database and literature by manual curation, and then reconstructed the whole signaling network diagram based on the collected information (see Section 3 for details). We reconstructed the AhR signaling pathway by including hypoxia and p53 pathways (Fig. 1). Then, we developed a mathematical model of this integrated system using ODEs (see Section 3).

To obtain the experimental data for parameter estimation, we used three different concentrations of TCDD dose input (0.1, 1 and 10 nM) to HepG2 cells and measured the expression levels of the downstream target genes (*CYP1A1* and *AhRR*) and the AhR localization patterns (Supplementary Fig. S1) at eight different time points over 52 h using immunoblot analysis. We also measured the expressions of the target genes (*VEGF* and *EGLN*) of HIF1α under hypoxia stimulation. All the kinetic parameters in our mathematical model were tuned to fit the experimental data (Fig. 2). We verified that the dose (TCDD)–response (AhR complex*n) curve predicted from our model is well in accord with the previous experimental report (Chen and Bunce, 2003) (Supplementary Fig. S2). Based on this, we further simulated the profiles of some key molecules under various conditions (Supplementary Figs S3–5) and investigated the crosstalk between TCDD and hypoxia pathways.

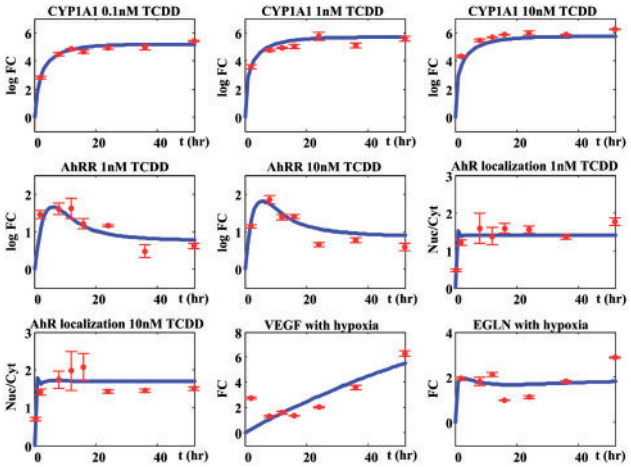

Fig. 2. Model fitting with experimental data. In all figures, blue lines denote computer simulation profiles, red circles indicate experimental data (FC denotes 'fold change'), and each error bar shows the standard error of each experimental data point.

4.2 Crosstalk between the TCDD and hypoxia pathways

In the foregoing section, we noted that both AhR and HIF1α commonly bind to ARNT and that this competitive binding can lead to crosstalk between them. To investigate the crosstalk effect in detail and to see how hypoxia affects the TCDD-induced signaling pathway, we have simulated AhR*/ARNT (* denotes TCDD-liganded) heterodimer concentration profile and its transcriptional activity through *CYP1A1* mRNA level under various hypoxia stimulations.

Without hypoxia (also called, 'normoxia'), both AhR*/ARNT and CYP1A1 increase rapidly and arrive at high steady-state levels under all different TCDD treatments (blue lines in Fig. 3), whereas they arrive at lower steady-state levels under a hypoxia condition. Moreover, we found that the decrease was slow and the steady-state level difference was small under a low hypoxia condition (green dashed lines in Fig. 3), whereas the decrease was fast and the steady-state level difference was large under a high hypoxia condition (red dot-dashed lines in Fig. 3).

We have also investigated the inverse relationship, i.e. the crosstalk effect of TCDD on HIF1α target gene expression (*VEGF* and *EGLN* induced by hypoxia). Without any stimulation, no transcription was induced (blue line for *VEGF* and red line for *EGLN* in the left panels of Fig. 4). With hypoxia stimulation, HIF1α protein was activated and the expressions of its target genes, *VEGF* and *EGLN*, were rapidly induced (middle panels in Fig. 4). Although HIF1α has strong effects on AhR localization and its target gene transcription via the limiting factor, ARNT, the crosstalk partner

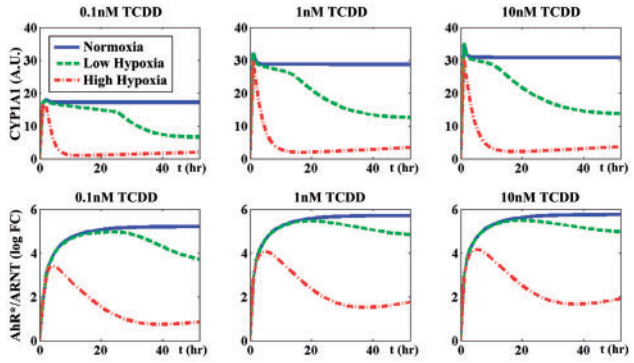

Fig. 3. Simulation results under various conditions (different levels of TCDD inputs and hypoxia conditions) showing the inhibitory effect of AhR target gene expression. For all different TCDD concentrations, we found that AhR*/ARNT and its target gene, CYP1A1 are repressed under the hypoxia condition and that such repression becomes stronger under a higher hypoxia condition.

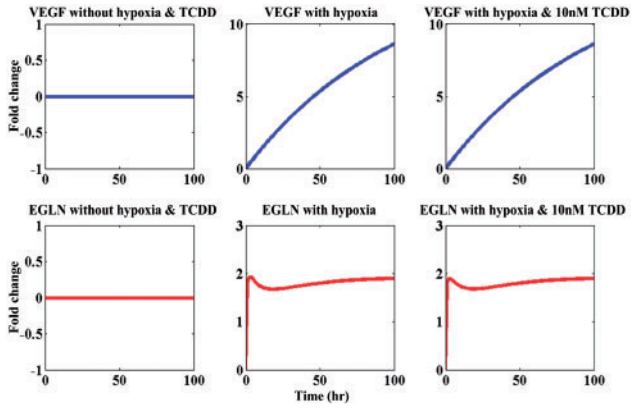

Fig. 4. Computer simulations of the HIF1α target gene expression under different conditions of hypoxia and 10 nM TCDD stimulation. Target genes of HIF1α, *VEGF* and *EGLN*, are transcribed only if hypoxia happens (middle panel in both rows). TCDD does not show any inhibitory effect on the transcription of HIF1α target genes that are induced by hypoxia (compare middle and right panels).

AhR has no significant effect on HIF1α target gene expression (right panels in Fig. 4). We have further investigated the dose–response characteristics by comparing the baseline (no crosstalk) model, the hypoxia crosstalk model, and the ARNT over-expression model (Supplementary Fig. S6). The hypoxia crosstalk model showed a similar dose–response characteristic with the baseline model, whereas the TCDD–CYP1A1 dose–response curve was shifted to left when ARNT is over-expressed (note that the dose–response curves were normalized with the maximum response levels for comparison of activation thresholds). This implies that the ARNT level rather than the hypoxia condition is more crucial in determining the dose–response characteristic of TCDD and CYP1A1.

We have further validated our simulation results by conducting experiments on target gene expressions. In particular, to confirm the simulation results on the crosstalk between HIF1α and AhR, we have probed the expression profiles of *CYP1A1* and *VEGF*. After HepG2 cells were treated with TCDD (10 nM) under both

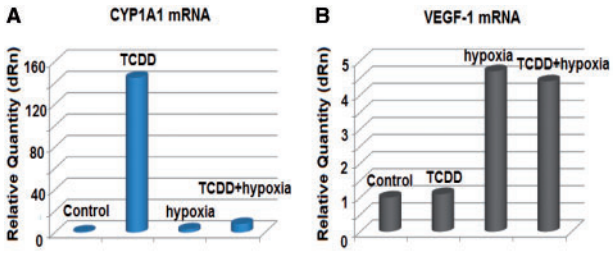

Fig. 5. Validation of the crosstalk between hypoxia and TCDD by comparing target gene expressions. After HepG2 cells were treated with TCDD (10 nM) under normoxic/hypoxic condition for 24 h, *CYP1A1* and *VEGF-1* mRNAs that are the target genes of AhR and HIF1α, respectively, were measured. One of the AhR target gene, *CYP1A1*, highly induced by TCDD was inhibited dramatically with hypoxic stimulation (**A**). HIF1α target gene, *VEGF-1* induced by hypoxia was not repressed by TCDD (**B**).

normoxic and hypoxic conditions for 24 h, total RNA extraction and cDNA synthesis were carried out (see Section 3 for details). To measure the levels of *CYP1A1* and *VEGF-1* mRNAs, real-time quantitative RT–PCR was performed using synthesized cDNA. The relative quantity was then calculated using the ΔΔCt method with *GAPDH* mRNA as an internal control. As in the simulation results, *CYP1A1* mRNA was sensitively up-regulated with TCDD input. With both hypoxia and TCDD treatment, the regulation of *CYP1A1* was, however, completely inhibited (Fig. 5A). *VEGF*, one of the well-known target genes induced by hypoxia stimulation, was also tested. *VEGF* was highly induced by hypoxia, distinct from TCDD input and control experiments. However, when both inputs were taken, unlike *CYP1A1*, *VEGF* was seldom inhibited (Fig. 5B).

The crosstalk between TCDD and hypoxia seems to be from the competition between their downstream signaling proteins, AhR and HIF1α, for binding with their co-partner, ARNT. The most interesting point is that TCDD did not affect the hypoxia pathway although the expression of *CYP1A1*, the target gene of AhR/ARNT, was strongly inhibited by hypoxia. This is different from many other well-known crosstalks in which signals are usually inhibited by each other. It might be because of either the *binding affinity* difference of AhR and HIF1α with respect to ARNT or the *limited concentration* of ARNT that actually forms this 'one-way' crosstalk. The stronger binding affinity to ARNT the protein has, the easier it is to win the competition and to remain forming a heterodimer with limited concentration of ARNT. In addition, we found that any increase or decrease of the total amount of ARNT from the basal level of our model (40 A.U.) can weaken this crosstalk effect (Supplementary Fig. S7). This implies that the crosstalk effect can be easily repressed by changing the protein level of ARNT.

Cells usually undergo transcriptional changes to maintain homeostasis against external stimuli. For instance, under hypoxia, cells lack dissolved oxygen and need to transcribe genes related to angiogenesis such as *VEGF* so as to supply sufficient oxygen. Therefore, HIF1α, the transcription factor of *VEGF,* is activated and the *VEGF* gene is transcribed. Under TCDD stimulus, cells turn on the AhR signaling pathway in order to respond to this stimulus by transcribing *CYP1A1*, which oxidizes a variety of compounds including steroids, fatty acid and xenobiotics (TCDD), and this response mechanism finally helps to digest out the compounds. On the other hand, if multiple stimuli are applied simultaneously, then

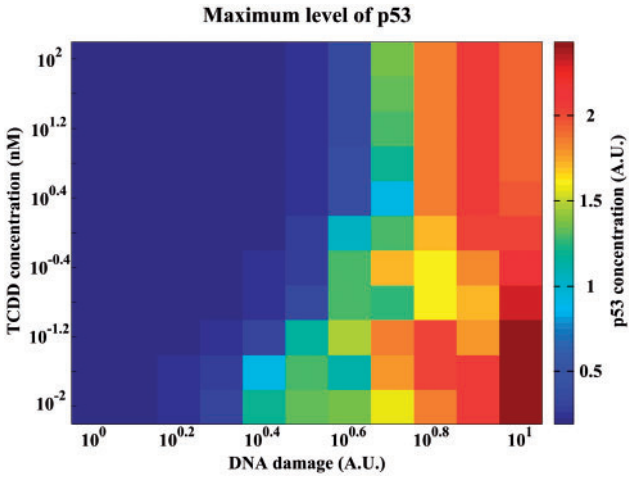

Fig. 6. Heat-map representation of the p53 activation level change with respect to TCDD concentration and DNA damage. TCDD intake represses the p53 response to DNA damage.

the situation becomes more complicated. In this case, a competition arises between the signaling proteins (HIF1α and AhR) and the shared protein (ARNT) is likely to bind more dominantly with the stronger signaling protein (HIF1α).

4.3 TCDD attenuates the p53 response

We have incorporated our AhR signaling pathway model with the p53 model of Zhang *et al*. (2008) based on the fact that TCDD input affects p53-related signals (i.e. when a TCDD treatment is given, the basal level of MDM2 abnormally increases and this makes the p53 level attenuated (Paajarvi *et al*., 2005)). We have investigated how TCDD input affects the p53 concentration under DNA damage using both simulations and experiments.

Figure 6 shows the maximum level changes of activated p53 with respect to various levels of TCDD concentration and DNA damage. This simulation result indicates that the p53 level becomes less sensitive to DNA damage if the concentration of TCDD increases. It also shows that p53 mostly remains at a basal level regardless of the TCDD concentration for low DNA damage, whereas the p53 response becomes attenuated along with the increase of TCDD concentration for high DNA damage. In particular, we note that the slightly induced p53 decreases to its basal level in the medium range ($10^{0.4}$–$10^{0.6}$ A.U.) of DNA damage due to the crosstalk between AhR and p53 signaling pathways.

The inhibitory effect of TCDD on the p53 activity is experimentally verified as follows. After HepG2 cells were incubated in the absence or presence of TCDD for 24 h, they were further treated with DOX for indicated times. Then, total cell lysates were prepared and subjected to immunoblot analysis against phospho-p53 (see Section 3 for details). Immunoblot analysis against GAPDH was done for equal protein loading. While without treating DOX, no phospho-p53 was observed, treating DOX showed the induction of phospho-p53 with either absence or presence of TCDD in cells. Under the presence of TCDD in cells, however, phospho-p53 was less observed than the case with TCDD (Fig. 7).

When DNA damage occurs, p53 is activated and transcribes its target genes for cell-cycle arrest, damage repairs, and apoptosis.

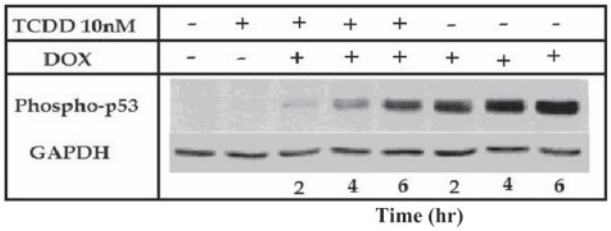

Fig. 7. TCDD inhibitiory effects on p53 phosphorylation under DNA damage. HepG2 cells were incubated for 24 h in the absence or presence of TCDD and they were further treated with DOX during the indicated period of time. Then, phospho-p53 (Ser-15) was measured.

As previously reported by Paajarvi *et al*. (2005), we also found that AhR, liganded by TCDD, inhibits the p53 activity from both experiments and computer simulations. In the case of p53 inhibition by TCDD-liganded AhR, p53 cannot properly supervise the transcriptional reactions against DNA damage and this causes a failure in recovering from the damage. This malfunctioning of p53 plus bare excretion of TCDD might eventually lead to TCDD-mediated carcinogenesis. In other words, TCDD weakens the functional activity of p53 as a killer to the damaged cells. Although the p53 activity is significantly inhibited by TCDD-liganded AhR, we found that the apoptosis rates are similar in both TCDD-treated and non-treated cases (Supplementary Fig. S8). We further performed computer simulations to investigate the change of hypothetical p53 'killer form' under various conditions such as all possible combination of TCDD treatment and DNA damage (see Supplementary Fig. S9). In summary, we found that the total concentration of apoptotic gene-transcribing p53 (p53 killer form) with TCDD treatment is similar to that without TCDD treatment under both mild and severe DNA damage although phosphorylated p53 is inhibited by TCDD treatment (see Supplementary Fig. S10).

5 CONCLUSION

To our knowledge, no attempt has been made to understand the complex regulatory mechanism of TCDD-mediated AhR pathway from an integrated system-level perspective. Only a few review papers described the overall schematic model of the AhR signaling pathway without consideration of the crosstalks (Barouki *et al*., 2007; Mimura and Fujii-Kuriyama, 2003). So, we have reconstructed a comprehensive model of the AhR signaling network through extensive manual curation, and developed a mathematical model of it using ODEs based on biochemical experiments. Our combined simulation analysis and experimental validation of the model showed that AhR localization and its transcriptional activity are dose-dependent and that they are influenced by hypoxia through the crosstalk with HIF1α where ARNT plays a role as a limiting factor. Interestingly, the hypoxia signaling inhibits the transcriptional activity of AhR, but the reverse is not true. This might be originated from the different binding affinities between AhR and ARNT, and HIF1α and ARNT. We also found that the maximum level of p53 changes as the levels of DNA damage and the TCDD intake vary. In particular, for low DNA damage, the p53 level does not change much along with the TCDD intake and remains at a basal level. For high DNA damage, TCDD attenuates the p53 response but the decrease is not enough and the transcription activity of p53 is

not fully inhibited. Interestingly, a weakly induced p53 activity is completely inhibited by TCDD-intake for a medium level of DNA damage. Taken together, our combined study provides us with a system-level understanding of the complicated cellular responses under various conditions. General limitations or challenges of our approach include the non-uniqueness problem of parameter estimates (i.e. the possibility of multiple parameter estimates that fit the given experimental data in a relatively similar degree) and the unknown missing component of the model. These can be alleviated by conducting more experiments or, conversely, these can motivate biologists to design new experiments.

Funding: National Research Foundation of Korea (NRF) grants funded by the Korea Government, the Ministry of Education, Science & Technology (MEST) (2009-0086964 and 2010-0017662); NiFDS (National Institute of Food and Drug Safety Evaluation) through the National Toxicology Program in Korea (KNTP).

Conflict of Interest: none declared.

REFERENCES

Barouki,R. *et al*. (2007) The aryl hydrocarbon receptor, more than a xenobiotic-interacting protein. *FEBS Lett.*, **581**, 3608–3615.

Chen,G. and Bunce,N.J. (2003) Polybrominated diphenyl ethers as Ah receptor agonists and antagonists. *Toxicol. Sci.*, **76**, 310–320.

Cho,K.H. *et al*. (2003) Investigations into the analysis and modeling of the TNF alpha-mediated NF-kappa B-signaling pathway. *Genome Res.*, **13**, 2413–2422.

Geva-Zatorsky,N. *et al.* (2006) Oscillations and variability in the p53 system. *Mol. Syst. Biol.*, **2**, 2006 0033.

Geyer,H.J. *et al.* (2002) Half-lives of tetra-, penta-, hexa-, hepta-, and octachlorodibenzo-p-dioxin in rats, monkeys, and humans—a critical review. *Chemosphere*, **48**, 631–644.

Gradin,K. *et al.* (1996) Functional interference between hypoxia and dioxin signal transduction pathways: competition for recruitment of the Arnt transcription factor. *Mol. Cell. Biol.*, **16**, 5221–5231.

Harris,S.L. and Levine,A.J. (2005) The p53 pathway: positive and negative feedback loops. *Oncogene*, **24**, 2899–2908.

Kanehisa,M. and Goto,S. (2000) KEGG: kyoto encyclopedia of genes and genomes. *Nucleic Acids Res.*, **28**, 27–30.

Kim,D. *et al.* (2009) Multiple roles of the NF-kappaB signaling pathway regulated by coupled negative feedback circuits. *FASEB J.*, **23**, 2796–2802.

Kim,D. *et al.* (2007) A hidden oncogenic positive feedback loop caused by crosstalk between Wnt and ERK pathways. *Oncogene*, **26**, 4571–4579.

Kim,J. *et al.* (2008) Evolutionary design principles of modules that control cellular differentiation: consequences for hysteresis and multistationarity. *Bioinformatics*, **24**, 1516–1522.

Kim,J.R. *et al.* (2008) Coupled feedback loops form dynamic motifs of cellular networks. *Biophys. J.*, **94**, 359–365.

Kimbrough,R.D. *et al*. (1977) Epidemiology and pathology of a tetrachlorodibenzodioxin poisoning episode. *Arch. Environ. Health*, **32**, 77–86.

Kwon,Y.K. and Cho,K.H. (2008) Coherent coupling of feedback loops: a design principle of cell signaling networks. *Bioinformatics*, **24**, 1926–1932.

Lahav,G. *et al*. (2004) Dynamics of the p53-Mdm2 feedback loop in individual cells. *Nat. Genet.*, **36**, 147–150.

Livak,K.J. and Schmittgen,T.D. (2001) Analysis of relative gene expression data using real-time quantitative PCR and the 2(-Delta Delta C(T)) Method. *Methods*, **25**, 402–408.

Longnecker,M.P. and Michalek,J.E. (2000) Serum dioxin level in relation to diabetes mellitus among Air Force veterans with background levels of exposure. *Epidemiology*, **11**, 44–48.

Mimura,J. and Fujii-Kuriyama,Y. (2003) Functional role of AhR in the expression of toxic effects by TCDD. *Biochim. Biophys. Acta*, **1619**, 263–268.

Paajarvi,G. *et al*. (2005) TCDD activates Mdm2 and attenuates the p53 response to DNA damaging agents. *Carcinogenesis*, **26**, 201–208.

Pavuk,M. *et al*. (2003) Serum 2,3,7,8-tetrachlorodibenzo-p-dioxin (TCDD) levels and thyroid function in Air Force veterans of the Vietnam War. *Ann. Epidemiol.*, **13**, 335–343.

Pirkle,J.L. *et al.* (1989) Estimates of the half-life of 2,3,7,8-tetrachlorodibenzo-p-dioxin in Vietnam Veterans of Operation Ranch Hand. *J. Toxicol. Environ. Health*, **27**, 165–171.

Pollenz,R.S. *et al*. (1999) Analysis of aryl hydrocarbon receptor-mediated signaling during physiological hypoxia reveals lack of competition for the aryl hydrocarbon nuclear translocator transcription factor. *Mol. Pharmacol.*, **56**, 1127–1137.

Reisdorph,R. and Lindahl,R. (2001) Aldehyde dehydrogenase 3 gene regulation: studies on constitutive and hypoxia-modulated expression. *Chem. Biol. Interact.*, **130–132**, 227–233.

Safe,S. (2001) Molecular biology of the Ah receptor and its role in carcinogenesis. *Toxicol. Lett.*, **120**, 1–7.

Shin,S.Y. *et al*. (2009) Positive- and negative-feedback regulations coordinate the dynamic behavior of the Ras-Raf-MEK-ERK signal transduction pathway. *J. Cell Sci.*, **122**, 425–435.

Shin,S.Y. *et al*. (2008) System-level investigation into the regulatory mechanism of the calcineurin/NFAT signaling pathway, *Cell Signal.*, **20**, 1117–1124.

Van den Berg,M. *et al*. (1998) Toxic equivalency factors (TEFs) for PCBs, PCDDs, PCDFs for humans and wildlife. *Environ. Health Perspect.*, **106**, 775–792.

Van den Berg,M. *et al.* (2006) The 2005 World Health Organization reevaluation of human and Mammalian toxic equivalency factors for dioxins and dioxin-like compounds. *Toxicol. Sci.*, **93**, 223–241.

Zhang,M. *et al*. (2008) Apparently low reproducibility of true differential expression discoveries in microarray studies. *Bioinformatics*, **24**, 2057–2063.

Zhang,T. *et al*. (2007) Exploring mechanisms of the DNA-damage response: p53 pulses and their possible relevance to apoptosis. *Cell Cycle*, **6**, 85–94.